Quaternary Science Reviews 26 (2007) 56–69

Plio–Pleistocene climate evolution: trends and transitions in glacial cycle dynamics

Lorraine E. Lisiecki*, Maureen E. Raymo

Department of Earth Sciences, Boston University, Boston, MA, USA

Received 21 November 2005; accepted 24 September 2006

Abstract

We describe the evolution of climate system dynamics by examining the climate response to changes in obliquity and precession over the last 5.3 Myr. In particular, we examine changes in the shape of glacial cycles and the power of obliquity and precession response in benthic $\delta^{18}O$. When the exponential trend in $\delta^{18}O$ variance is removed, its spectral power exhibits strong, proportional responses to amplitude modulations in orbital forcing over most of the Plio–Pleistocene. Precession responses correlate with modulations in forcing for the last 5 Myr, but 41-kyr response is sensitive to obliquity modulation only before 1.4 Myr. Where responses are sensitive to modulations in forcing, we demonstrate that glacial cycles are orbitally forced rather than being self-sustained or paced by orbital changes. The shapes of glacial cycles have several nonlinear properties, which may be indicative of glacial–interglacial differences in climate sensitivity or response time. The "saw-tooth" asymmetry of glacial cycles first appears shortly after the onset of major northern hemisphere glaciation, and the relative duration of interglacial stages decreases at 1.4 Myr. Collectively, trends in the shape of glacial cycles and the sensitivity of $\delta^{18}O$ to obliquity and precession are suggestive of major transitions in climate dynamics at approximately 2.5 and 1.4 Myr but show no significant change associated with the appearance of strong 100-kyr cycles during the mid-Pleistocene transition.

1. Introduction

1.1. Plio–Pleistocene climate change

Long-term trends of climatic cooling and increasing glacial cycle amplitude during the Plio–Pleistocene are suggestive of significant changes in the dynamics of the climate system, but the cause of these trends and the specific changes in glacial dynamics associated with them are poorly understood. Most Plio–Pleistocene climate research has focused on two relatively abrupt climate transitions, the onset of major northern hemisphere glaciation at approximately 2.7 Myr and the mid-Pleistocene transition (MPT) when the dominant periodicity of glacial response changes from 41 to ~100 kyr. However, the causes of even these well-studied transitions in glacial cycle dynamics remain uncertain.

For example, the tectonic closure of the Isthmus of Panama (Keigwin, 1982; Maier-Reimer et al., 1990), Tibetan uplift (Raymo et al., 1988; Rea et al., 1998), restriction of the Indonesian seaway (Cane and Molnar, 2001), shoaling of the thermocline (Philander and Fedorov, 2003), obliquity modulation (Haug and Tiedemann, 1998; Maslin et al., 1998), and changes in North Pacific stratification (Haug et al., 1999; Sigman et al., 2004) have all been proposed as mechanisms for the initiation of northern hemisphere glaciation. A long-term cooling trend is often considered responsible for the change in glacial dynamics at the MPT. Mechanisms proposed for this transition include changes in sea ice formation (Tziperman and Gildor, 2003; Ashkenazy and Tziperman, 2004), a switch from terrestrial to marine ice margins in Antarctica (Raymo et al., 2006), a gradual increase in the insolation threshhold for ice-sheet ablation (Raymo, 1997; Paillard, 1998; Berger et al., 1999; Huybers, 2006), and changes in ice-sheet stability due to the gradual erosion of North American regolith (Clark and Pollard, 1998). A better description of glacial response changes throughout the

*Corresponding author. Tel.: +1 617 358 4620.
E-mail address: lisiecki@bu.edu (L.E. Lisiecki).

0277-3791/$ - see front matter © 2006 Elsevier Ltd. All rights reserved.
doi:10.1016/j.quascirev.2006.09.005

Plio–Pleistocene could help constrain the possible causes of change in climate dynamics.

1.2. Outline

We quantify the evolution of glacial cycle dynamics over the Plio–Pleistocene using several characteristics of the climate response to cyclic changes in the Earth's orbital configuration. Climate responses to obliquity and precession are traditionally considered linear (e.g., Hagelberg et al., 1991; Imbrie et al., 1992; Tiedemann et al., 1994) because many climate records covary with insolation changes due to these orbital parameters, usually with a small phase lag. Such a linear response would be ideal for identifying changes in the climate system because it implies a simple relationship between the climate's input and output. However, several recent studies (e.g., Ashkenazy and Tziperman, 2004; Huybers and Wunsch, 2004; Huybers, 2007) have proposed that obliquity and/or precession responses are strongly nonlinear for some or all of the last 5 Myr. By developing a detailed comparison of orbital forcing and climate response, we can better constrain the physics of glacial dynamics and the sources of long-term trends and transitions in climate response.

Below we present our strategy of comparing obliquity and precession forcing with a global climate signal in order to reconstruct changes in glacial cycle dynamics. Section 2 provides details about the record used as a proxy for global climate response. We then measure power in the frequency bands of obliquity and precession (Section 3) as well as two metrics of glacial cycle shape (Section 4) in climate forcing and response. Section 5 uses these observations to classify the dynamics of obliquity and precession responses. Section 6 discusses the implications of observed trends and transitions for the evolution of Plio–Pleistocene glacial cycle dynamics. Finally, we summarize our findings in Section 7.

1.3. Glacial cycle dynamics

In this study, we analyze the dynamics of the climate system as a whole by comparing orbital forcing inputs with a single global "output." The inputs used are the orbital parameters of obliquity and precession (Laskar et al., 1993), which control both the spatial and seasonal distribution of incoming solar radiation. The output, benthic $\delta^{18}O$, is intended as a measure of mean climate state (see Section 2) and results from the complex interactions of many climate system components responding to changes in the inputs. In the context of this highly simplified conceptual model, obliquity and precession responses are typically considered linear.

Here, the term linear is a simplification referring to the ability of a linear system to describe climate response on a particular timescale (King, 1996). We adopt this definition for the following discussion but acknowledge that many aspects of climate response are nonlinear. For example, the Milankovitch theory that glacial cycles are driven by summer insolation at 65°N relies on a well-known nonlinearity in the sensitivity of ice sheets to insolation over the annual cycle (e.g., Denton et al., 2005). Positive feedbacks, such as those involving ice albedo or greenhouse gas concentrations, provide additional sources of nonlinearity in the climate system. The reader is referred to King (1996) for an extensive discussion on how to identify linear and nonlinear responses in climate data.

If the climate system were a stationary linear system, the amplitude modulation and cycle shape of its input and output would match. Observed differences between the input and output could result from nonlinearity or nonstationarity (i.e., changes in the system's properties over time). We test whether obliquity and precession responses are consistent with a linear system by measuring amplitude modulation and cycle shape and determining whether any differences between the input and output are best explained by nonlinearity or nonstationarity. Because the global cooling trend and increase in glacial cycle amplitude during the Plio–Pleistocene are strongly suggestive of a nonstationary system, we attempt to identify simple relationships that resolve the differences between input and output and thereby reconstruct changes in glacial dynamics.

We also compare the observed climate response with several nonlinear climate models, which have different implications for amplitude modulation in the climate record. Piecewise linear models (e.g., Imbrie and Imbrie, 1980; Paillard, 1998) are nonlinear because the sensitivity or response time of the climate system varies as a function of climate state within the glacial cycle. These models alter the shape of glacial cycles (e.g., producing an asymmetric response), but their output is still sensitive to amplitude modulations in orbital forcing because changes in insolation directly drive climate change. In contrast, models of self-sustained variability or orbital pacing (Gildor and Tziperman, 2000; Ashkenazy and Tziperman, 2004; Huybers, 2007) display little sensitivity to the power of orbital forcing because orbital changes only trigger changes in the glacial state. Therefore, a comparison of amplitude modulation in forcing and response can determine whether a piecewise linear or orbital pacing model is more consistent with the Plio–Pleistocene climate record.

2. The climate signal

Benthic $\delta^{18}O$ is a common proxy for high-latitude climate response because it measures changes in global ice volume and deep water temperatures, which are controlled by high-latitude surface temperatures and tend to be quite uniform. We use an average of 57 benthic $\delta^{18}O$ records (Lisiecki and Raymo, 2005; hereafter referred to as the LR04 stack) as our climate response signal. The LR04 stack is particularly well-suited for this analysis because it is a 5.3-Myr, globally averaged record with a high signal-to-noise ratio and a resolution of 1–5 kyr.

The LR04 stack is orbitally tuned to a simple ice model (Imbrie and Imbrie, 1980) driven by June 21 insolation at

65°N (Laskar et al., 1993). However, the stack's age model is also constrained by average sedimentation rates to prevent overtuning. The LR04 stack and age model are generally consistent with the SPECMAP stack (Imbrie et al., 1984), the depth-derived age model of Huybers and Wunsch (2004), and a 6-Myr composite of benthic $\delta^{18}O$ records from three sites (V19-30, ODP 677, and ODP 846) (Shackleton, 1995). However, the results presented in this study are not highly sensitive to age model uncertainty because values are averaged over windows of 320 and 400 kyr. (These window sizes are selected to include an even multiple of 40-kyr cycles. In all figures, values are plotted at the center of the window over which they are calculated.)

Results are also presented for the LR04 stack with an alternate age model that has no orbital tuning. This age model is generated by assuming a constant average sedimentation rate for all component $\delta^{18}O$ records between tie points generated by graphic correlation (Lisiecki and Lisiecki, 2002) with ~10-kyr spacing. (Ages are only fixed at the stack's endpoints at 0 and 5.3 Myr. Sedimentation rates are set to be 9% higher from 0 to 700 kyr to compensate, in a greatly simplified way, for the effects of sediment compaction down core.) This constant sedimentation rate model differs from the LR04 age model by less than 40 kyr across the entire Plio–Pleistocene. We demostrate that the untuned age model produces similar results for the amplitude modulation of orbital responses and the shape of glacial cycles, indicating that our conclusions are robust with respect to age model uncertainty and that they are not artifacts of orbital tuning. The results presented in this study use the original, tuned LR04 age model except where otherwise noted.

3. Amplitude modulation

There are several ways in which the climate response to orbital forcing can be quantified. One common metric is gain, which measures the ratio of response amplitude to forcing amplitude at a given frequency. The gain of a stationary linear system can be large or small but must be constant as the amplitude of forcing varies, producing a perfect correlation between the power of forcing and response. Therefore, we measure the correlation coefficient of power versus time for the frequencies of obliquity and precession as one metric of a linear response. We use the term sensitivity to distinguish the relative response power from the relative response amplitude defined by gain. In Section 3.4 we also define modulation sensitivity, which describes the amount of modulation in climate response relative to the modulation in forcing.

3.1. Detrending the response

To distinguish between a nonstationary system and a nonlinear one, we attempt to identify simple trends in sensitivity that produce a good correlation between forcing and response. This is an important step because the climate is undoubtably nonstationary over the last 5 Myr as evidenced by a long-term cooling trend and a long-term increase in glacial amplitudes. First, we find a single, long-term trend that might describe changes in the sensitivity of both obliquity and precession. Later, we consider other trends that might better describe the individual orbital responses. The ability to identify a relatively simple trend in sensitivity that produces a good correlation between forcing and response would be consistent with a nonstationary linear response and would quantify changes in the dynamics of the climate system.

The mean and variance of benthic $\delta^{18}O$ are calculated using a 320-kyr moving window (Fig. 1) in order to identify potential long-term trends in climate system response. The mean is indicative of average global ice volume and deep-water temperature, and the variance relates to the amplitude of glacial cycles. The increase in mean $\delta^{18}O$ is nearly linear, particularly from 2.5 to 0.8 Myr (Myr ago). The long-term trend in variance is well described over the entire Plio–Pleistocene by the exponential curve $0.22e^{-0.68t}$ (where t is time in millions of years before present).

Fig. 2a illustrates changes in the spectral power of $\delta^{18}O$ in three orbital bands, calculated by the squared fast Fourier transform (FFT) of a moving 400-kyr boxcar filter. The variance of all three orbital bands increases with time, despite the lack of a similar trend in orbital forcing. This suggests the presence of an amplifying mechanism which gradually increased the climate's sensitivity to orbital forcing and that the variance of $\delta^{18}O$ should be detrended before analyzing the relationship between forcing and response. We begin with the most conservative approach to detrending the data, which is to assume that all spectral bands experience the same trend in variance. In Sections 3.2 and 3.3, we evaluate other trends for obliquity and precession sensitivity based on comparisons of their individual forcing and response.

One way to detrend spectral power is to calculate the percent of variance found in each orbital band (Fig. 2b). This successfully removes the long-term trend in variance but is not ideal for characterizing the modulation of orbital responses for two reasons. First, the response in each orbital band is expected to be independent of the others, but changes in the power of one spectral band will affect the percent variance of all orbital bands. Second, in the same way that the percent variance calculation removes the overall trend in variance, it may also artificially weaken modulations.

A better detrending technique, shown in Fig. 2c, is to divide the variance in each orbital band by a smooth model of total variance, in this case the best-fit exponential curve from Fig. 1. This removes the nonstationary character of the data without allowing short-term changes in one spectral band to distort the others or weakening modulations in spectral power. In practice, the percent variance and exponentially detrended variance are fairly similar due to the presence of power outside of these orbital bands.

Fig. 3 compares the exponentially detrended power of climate response in the 41-, 23-, and 19-kyr frequency bands

using the LR04 age model and the alternate, untuned age model with constant sedimentation rate. (Throughout this paper, unless otherwise noted, we integrate power over the frequency ranges of 1/43–1/38 kyr^{-1} for obliquity, 1/25–1/21 kyr^{-1} for the 23-kyr precession band, and 1/20–1/18 kyr^{-1} for the 19-kyr precession band.) The pattern of modulation for both age models is very similar in the 41- and 23-kyr bands if we use slightly wider frequency bands for the untuned age model (see figure caption). The power of the two age models differs slightly in the 19-kyr band, presumably due to the low signal-to-noise ratio at this frequency. Based on these comparisons, we assert that our analyses of amplitude modulation are not strongly dependent on the age model of the LR04 stack and are not an artifact of orbital tuning.

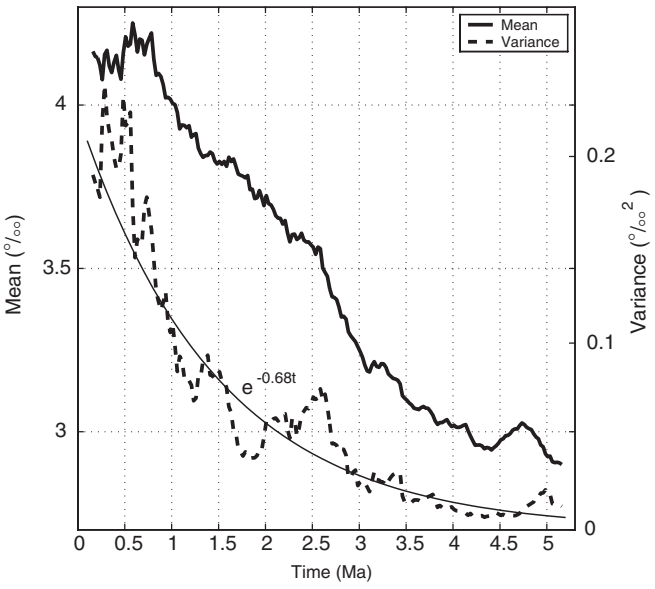

Fig. 1. 320-kyr moving averages of benthic $\delta^{18}O$ mean and variance. Also plotted is the best-fit exponential curve of variance (thin line).

3.2. Obliquity

In Fig. 4a, the exponentially detrended 41-kyr power of $\delta^{18}O$ is compared to normalized modulations in the power of obliquity forcing. Over the Plio–Pleistocene the two curves have a correlation r of 0.68. Before 1.4 Myr the detrended 41-kyr power of $\delta^{18}O$ matches the modulation of obliquity power extremely well, with a correlation of 0.87 from 5.3 to 1.4 Myr. At 1.4 Myr the detrended obliquity response drops and subsequently exhibits almost no modulation, resulting in a lack of correlation ($r = 0.02$) between the 41-kyr power of forcing and detrended response from 1.4 to 0 Myr.

Now the fit between forcing and response detrended by the exponential curve (as in Fig. 4a) is compared to the fit when response is detrended by other simple functions. First, we try modeling the increase in obliquity sensitivity as linear from 5.3 to 1.4 Myr. A linearly detrended response produces a maximum correlation in 41-kyr power from 5.3 to 1.4 Myr of 0.75 compared to 0.87 for the exponential trend. Next, we model a transition in obliquity sensitivity by using two linear trends so as to optimize the correlation between obliquity forcing and response over the entire 5.3 Myr. The best fit for this two-part linear trend is produced by an increase in

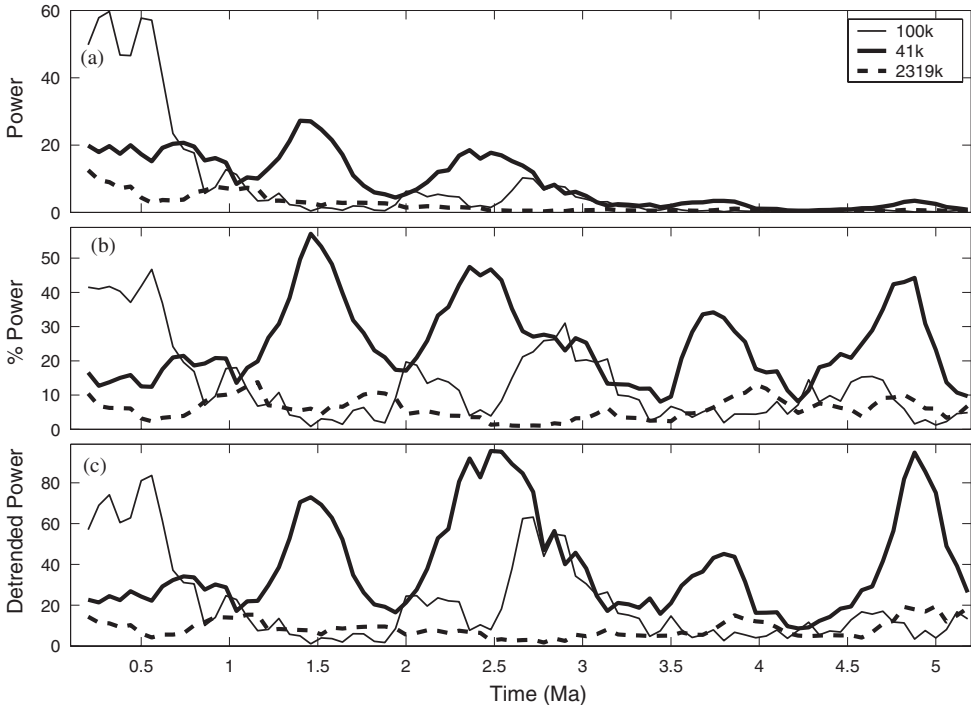

Fig. 2. (a) Spectral power (with arbitrary scale) of benthic $\delta^{18}O$ in the frequency bands for eccentricity (89–126 kyr), obliquity (38–43 kyr), and precession (18–25 kyr). (b) Percent of total power in each orbital band. (c) Power detrended by the exponential $e^{-0.68t}$ (see text).

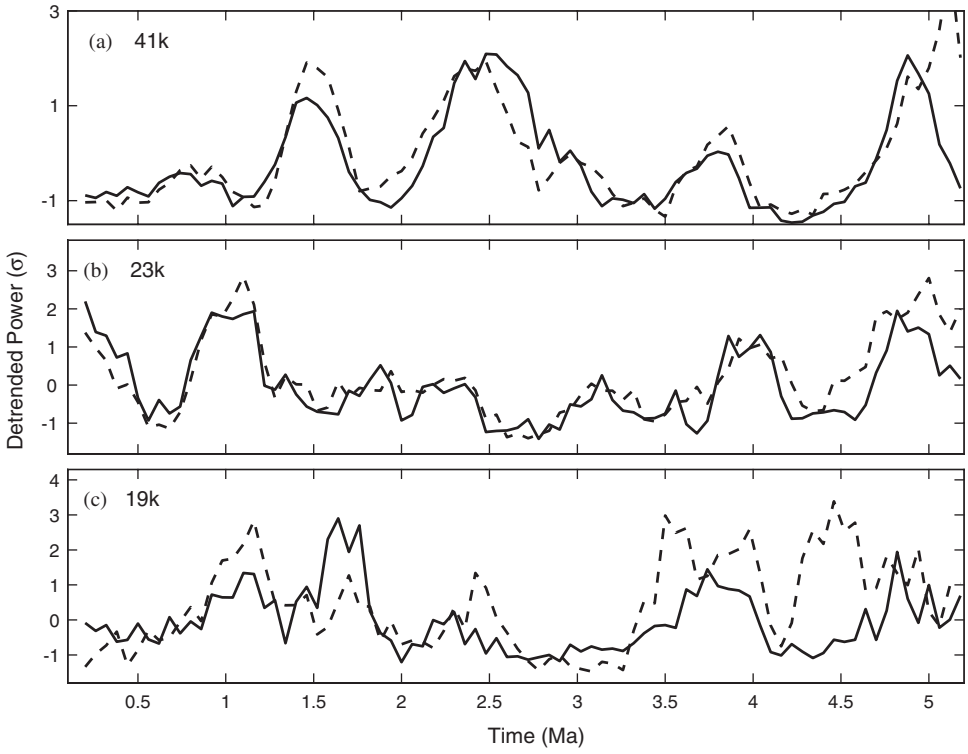

Fig. 3. Age model comparison of the detrended power in benthic $\delta^{18}O$ for (a) obliquity, (b) 23-kyr precession, and (c) 19-kyr precession. The LR04 age model (solid line) and an age model with constant average sedimentation rate (dotted line) produce similar results. All responses are exponentially detrended by $e^{-0.68t}$ from 5.3 to 0 Myr and normalized to zero mean and unit standard deviation for 3–0 Myr. For the age model with constant sedimentation rate, we use expanded frequency bands of 1/47–1/36 kyr^{-1} for 41-kyr response and 1/27–1/21 kyr^{-1} for 23-kyr response to compensate for lack of tuning.

obliquity sensitivity from 5.3 to 1.8 Myr followed by a decrease from 1.8 to 0 Myr. Detrending with this sensitivity model generates a correlation of 0.71 for the entire Plio–Pleistocene and correlations of 0.79 for 5.3–1.4 Myr and 0.28 for 1.4–0 Myr. Based on the correlation coefficients, the exponential trend provides the best fit between forcing and response from 5.3 to 1.4 Myr, suggesting that the exponential form is a meaningful description of the change in obliquity sensitivity. Results based on the two-part linear trend also confirm that 41-kyr response is poorly correlated to changes in the power of forcing after 1.4 Myr.

By measuring the obliquity gain of climate response as the ratio of 41-kyr amplitude in $\delta^{18}O$ and insolation, Ravelo et al. (2004) proposed that obliquity sensitivity gradually increased from 4 to 2 Myr and peaked from 2.0 to 0.6 Myr. Fig. 5a shows similar results when the same calculation is performed with the LR04 benthic stack, but a conceptual model of enhanced obliquity gain in the early Pleistocene does not address the fact that the amplitudes of obliquity forcing and response are uncorrelated from 1.4 to 0 Myr. This lack of correlation may indicate that obliquity is not driving 41-kyr glacial cycles after 1.4 Myr, only pacing them (see Section 5.1). Because gain would not be a physically meaningful description of climate response after 1.4 Myr if glacial cycles are no longer forced by obliquity, we propose an alternate description of obliquity sensitivity, which is illustrated in Fig. 5b. We observe an exponential increase in the obliquity gain of $\delta^{18}O$ from 5.3 to 1.4 Myr, followed by a decrease in 41-kyr response and near-zero correlation ($r = 0.04$) between the amplitudes of obliquity forcing and response from 1.4 to 0 Myr. Since 1.1 Myr, the amplitude of 41-kyr response (not detrended) is nearly constant with a mean value that is 66% of its maximum at 1.47 Myr. A local minimum in 41-kyr power occurs at ~1.2 Myr, which may be a short-term response to climate reorganization or an effect of random variability.

3.3. Precession

In the precession bands, detrending based on the exponential increase in total variance produces correlations between forcing and response of 0.49 and 0.52 in the 23- and 19-kyr bands, respectively. Although these values are smaller than the correlation for detrended obliquity response, sensitivity to precession modulation appears to persist throughout the Plio–Pleistocene. The smaller correlations for precession may result from the weak spectral power of $\delta^{18}O$ at those frequencies, which makes their measurement more susceptible to noise. However, the conservative assumption that climate sensitivity to precession follows the same trend as total variance may also be overly simplistic, as suggested by the fact that the undetrended 23-kyr power of $\delta^{18}O$ (not shown) does not display a long-term increase until about 2.5 Myr.

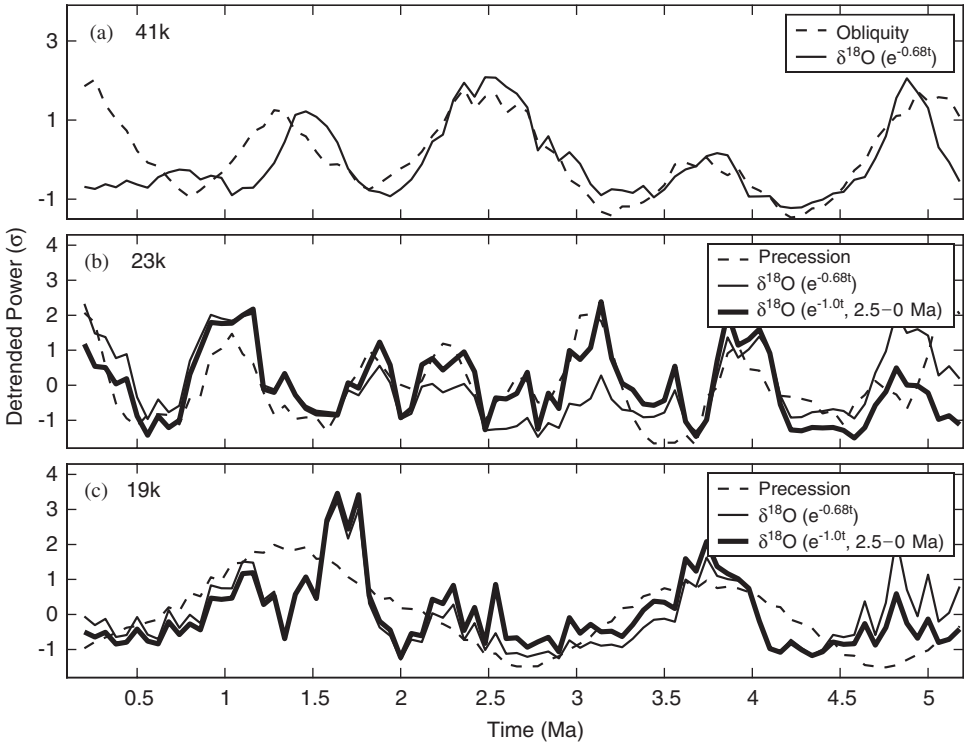

Fig. 4. Orbital forcing and benthic $\delta^{18}O$ response for (a) obliquity, (b) 23-kyr precession, and (c) 19-kyr precession. All curves are plotted with zero mean and unit standard deviation. All three responses are shown detrended by $e^{-0.68t}$ from 5.3 to 0 Myr (thin line). The 23- and 19-kyr responses are also shown detrended for a 90% increase in power at 2.5 Myr and an exponential increase of $e^{-1.0t}$ from 2.5 to 0 Myr (thick line).

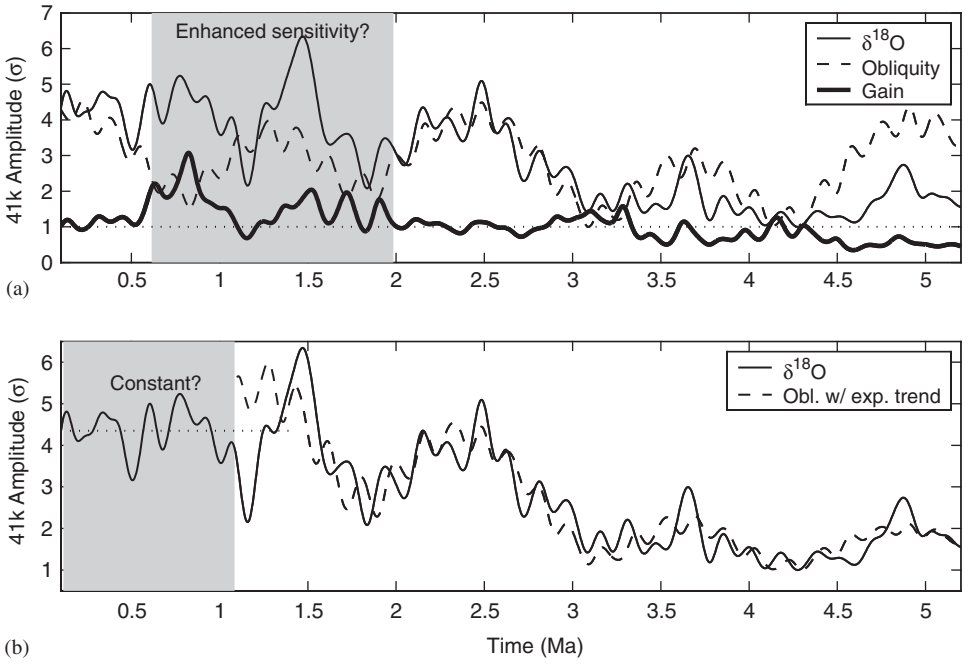

Fig. 5. Obliquity gain. (a) Ravelo et al. (2004) describe an interval of maximum obliquity sensitivity from 2 to 0.6 Myr. However, the amplitudes of 41-kyr forcing and response are poorly correlated over most of this interval. (b) 41-kyr response is well modeled by an exponential increase in obliquity gain from 5.3 to 1.4 Myr and a constant 41-kyr amplitude after 1.1 Myr. (The 41-kyr amplitudes of benthic $\delta^{18}O$ and obliquity are calculated by complex demodulation and have no detrending. All curves except gain are scaled based on their standard deviation from 5.2 to 2.0 Myr and assigned a minimum value of unity. Gain is the ratio of the scaled amplitudes of $\delta^{18}O$ and obliquity.)

We construct an alternate simple model of precession sensitivity by optimizing the correlation between detrended 23-kyr response and precession forcing. In this optimal model (thick lines in Fig. 4b and c), precession sensitivity is constant before 2.5 Myr, increases by 90% at 2.5 Myr, and subsequently increases at a rate of $e^{-10.t}$ (as before, t is time

in Myr before present). This increases the correlation coefficient for the 23-kyr band to 0.55 for the last 5.3 Myr and to 0.73 for the last 4.5 Myr. We conclude that, unlike the 41-kyr obliquity response, precession response displays an exponential increase in sensitivity and a correlation with modulations in forcing throughout the Pleistocene.

3.4. Modulation sensitivity

Because the correlation coefficient of power versus time is not sensitive to the degree of modulation in response relative to forcing, we additionally quantify and compare the amount of modulation in both signals. We define a normalized modulation amplitude A_{mod} as

$$A_{\mathrm{mod}} = \frac{P_{\max} - P_{\min}}{2\bar{P}}, \quad (1)$$

where $P_{\max}$ and $P_{\min}$ are power at a particular frequency measured at the times of maximum and minimum forcing within a modulation cycle. $\bar{P}$ is the mean power between the times of maximum and minimum forcing; using a short-term mean minimizes the effects of nonstationarity in the climate system. Aditionally, we define modulation sensitivity as the ratio of A_{mod} in response relative to forcing. A linear climate system would produce a modulation sensitivity of one. A very small modulation sensitivity would be produced by a system that has little response to changes in the power of forcing, such as models in which glacial cycles are only paced by orbital forcing. Finally, modulation sensitivities much larger than one could indicate the presence of positive feedbacks, which increase the climate's sensitivity as the power of forcing increases.

Although the amplitudes of Plio–Pleistocene obliquity cycles are fairly small, with obliquity ranging only from 22 to 24.5° (Laskar et al., 1993), the amplitude modulation of obliquity is quite strong. For example, the amplitude of obliquity cycles varies by a factor of five from 3.1 to 2.5 Myr, with minimum and maximum amplitudes of 0.25° and 1.25° respectively. In Table 1, we quantify A_{mod} and the modulation sensitivity for each of the five cycles of obliquity modulation in the Plio–Pleistocene. For both the unmodified and exponentially detrended obliquity responses, the modulation sensitivity of each cycle before 1.4 Myr is greater than or approximately equal to one. After 1.4 Myr the modulation sensitivity drops to near zero indicating a lack of sensitivity to forcing modulation.

Table 1 also provides the average modulation sensitivity for the 23- and 19-kyr precession bands calculated for both the unmodified response power and the response detrended by $e^{-1.0t}$ from 2.5 to 0 Myr. To compensate for the lower signal-to-noise ratio in precession response, we calculate the average modulation sensitivity from the ratio of A_{mod} for each modulation from 4.5 to 0 Myr (10 values in the 23-kyr band and 4 in the 19-kyr band). The modulation sensitivity of 1.1 in the 19-kyr band is consistent with a linear response, and the modulation sensitivity of 1.8 in the 23-kyr band is slightly higher than expected for a linear response. However, both values are consistent with direct forcing by precession (see Section 5.1).

4. Glacial cycle shape

Changes in climate dynamics are also suggested by changes in the shapes of glacial cycles. Cycle shapes are first measured in terms of asymmetry (Fig. 6) by comparing the average rates of warming and cooling in 320-kyr windows. These rates are calculated by separately averaging the positive and negative slopes of $\delta^{18}O$ over each 4-kyr interval that shows a trend of at least $\pm 0.01‰\,\mathrm{kyr}^{-1}$. Not surprisingly, the average rates of both warming and cooling increase as the amplitudes of glacial cycles increase. In the early and mid-Pliocene the absolute values of the two slopes are nearly identical, but beginning at 2.5 Myr the rate of deglaciation usually exceeds the rate of ice sheet growth (Fig. 6a). Several other studies (Raymo, 1992; Ashkenazy and Tziperman, 2004; Liu and Herbert, 2004; Huybers, 2007) have also observed asymmetry in late Pliocene and early Pleistocene glacial cycles. This asymmetry (measured as the ratio of deglacial to glacial slope in Fig. 6b) tends to increase with time, eventually creating the pronounced saw-tooth shape of late Pleistocene glacial cycles. The development of this asymmetry is most likely due to a change in the internal dynamics of the climate system because asymmetry is not found in any orbital or insolation curves.

Skewness is another metric of cycle shape, in this case measuring the relative duration of glacials and interglacials, with positive skewness indicating that interglacial conditions (defined by lighter than average values of $\delta^{18}O$) persist longer than glacial conditions (greater than average values of $\delta^{18}O$). Skewness is defined as the third central moment of a probability distribution and is calculated for a variable X by $E([X–E(X)]^3)$, where $E(X)$ denotes the expectation value or mean of X. Fig. 7 shows the skewness (measured in a 320-kyr moving window) of benthic $\delta^{18}O$ with both age models and of the simple ice model (Imbrie and Imbrie, 1980) used to tune the LR04 age model. Obliquity, precession, and 21 June insolation at 65°N all have zero skewness.

Large, positive skewness is observed in $\delta^{18}O$ from 4.2 to 1.6 Myr, indicating that Pliocene climate was dominated by interglacial conditions. At ~1.5 Myr skewness displays a step-like decrease, after which its average value is slightly negative. This is due to a decrease in the average duration of interglacials relative to glacials. Because the skewness calculation compares $\delta^{18}O$ values to their average within each 320-kyr window, this decrease in skewness is not an artifact of the long-term increase in $\delta^{18}O$. In a lower resolution study, Hagelberg et al. (1991) also observed a negative trend in the skewness of $\delta^{18}O$ since 2 Myr.

Table 1
Modulation sensitivity

Cycle (kyr)	Time (Myr)	Unmodified $\delta^{18}O$ A_{mod}[b]	Orbital A_{mod}[b]	Unmodified sensitivity	Detrended sensitivity[a]
41	4.9–4.2	0.81	0.92	0.87	1.09
	4.2–3.7	0.80	0.62	1.29	1.08
	3.2–2.4	0.81	0.70	1.15	0.84
	1.8–1.4	0.60	0.40	1.50	1.22
	1.3–0.8	−0.12	0.57	−0.21	0.16
	0.8–0.3	−0.04	0.68	−0.06	−0.33
23	4.5–0[c]	0.46	0.27	1.77	1.78
19	4.5–0[c]	0.75	0.74	1.06	1.07

[a]41-kyr response detrended by $e^{-0.68t}$ from 5.3 to 0 Myr. 23- and 19-kyr responses detrended by $e^{-1.0t}$ from 2.5 to 0 Myr. (Detrended A_{mod} not shown.).
[b]Normalized amplitude of power modulation, see Section 3.4.
[c]Average values for all modulations in age range.

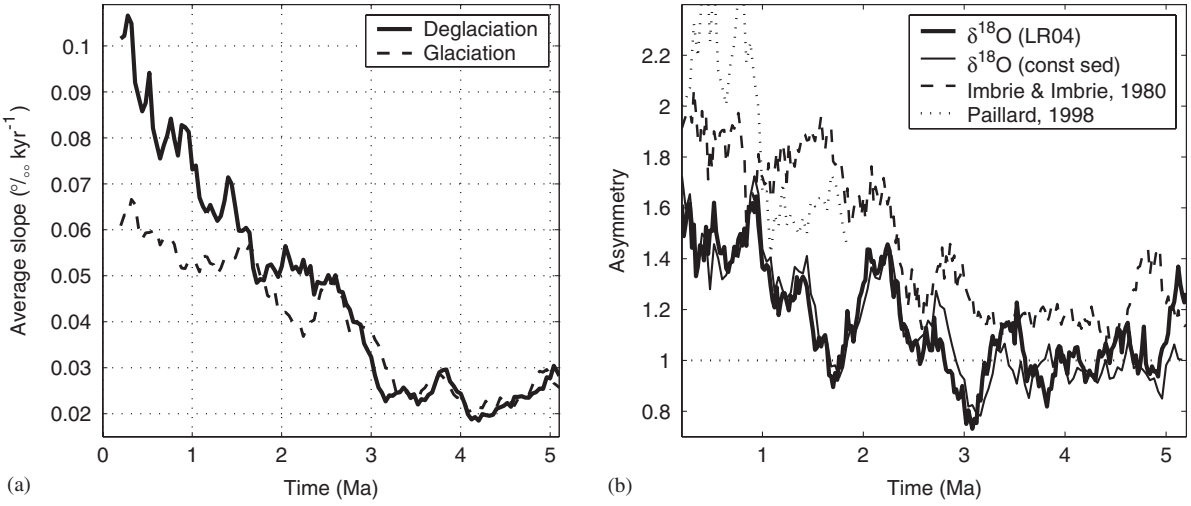

Fig. 6. Glacial asymmetry. (a) Absolute values of warming (deglaciation) and cooling (glaciation) slopes averaged over 320-kyr windows using the LR04 age model. (b) Asymmetry (absolute value of warming slope divided by cooling slope) for the $\delta^{18}O$ record using both the LR04 and constant sedimentation rate age models. Also shown is the asymmetry produced by two piecewise linear ice models, the Imbrie and Imbrie (1980) model with nonstationary parameterizations (Lisiecki and Raymo, 2005) and the 2-Myr nonstationary model of Paillard (1998).

5. Dynamics of orbital responses

5.1. Constraints of amplitude modulation

Comparing the amplitude modulation of obliquity and precession with the modulation of 41-, 23-, and 19-kyr power in $\delta^{18}O$ provides insight into the mechanisms generating these responses. In this section, we evaluate whether glacial responses are driven directly (and possibly linearly) by obliquity and precession, only paced by orbital change (e.g., Ashkenazy and Tziperman, 2004; Huybers, 2007), or produced as nonlinear combinations of other frequencies (e.g., Huybers and Wunsch, 2004). Direct orbital forcing should be distinguishable from these nonlinear indirect mechanisms based on the modulation sensitivity of climate response.

Sections 3.2 and 3.3 demonstrate the good correlation between modulations in forcing and detrended response for obliquity and precession over most of the Plio–Pleistocene, and Section 3.4 measures the climate's sensitivity to these modulations. A linear climate system would have a modulation sensitivity of 1 because the percent change in the power of response would match the percent change in forcing. Self-sustained oscillations, which are only paced by orbital cycles, would have little or no response to changes in the power of forcing and hence a very small modulation sensitivity. Similarly, a response generated by the nonlinear interactions of other frequencies would have an average modulation sensitivity near zero because the amplitudes of climate response and orbital forcing would not be correlated. For example, if 23-kyr response is generated by the nonlinear interaction of 41- and 100-kyr cycles

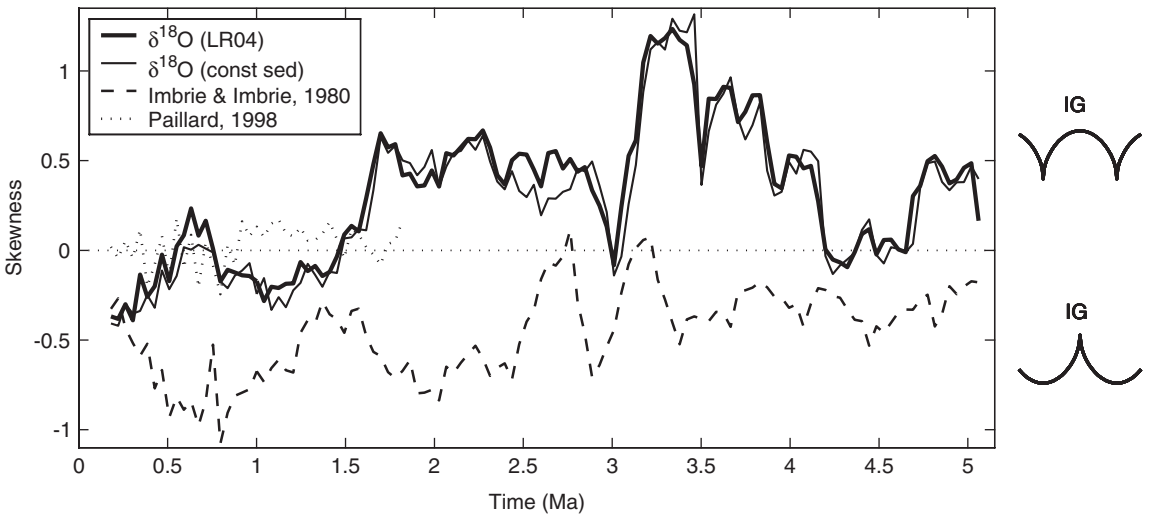

Fig. 7. Skewness of $\delta^{18}O$ for the LR04 and constant sedimentation rate age models and the skewness of two piecewise linear ice models, the Imbrie and Imbrie (1980) model with nonstationary parameterizations (Lisiecki and Raymo, 2005) and the 2-Myr nonstationary model of Paillard (1998). Skewness is measured on a normalized scale in 320-kyr windows. Also shown are examples of glacial cycles with positive (top) and negative (bottom) skewness.

$(1/41 + 2/100 = 1/23)$ as proposed by Huybers and Wunsch (2004), the 23-kyr power of $\delta^{18}O$ would be uncorrelated to precession modulation (if the 100-kyr cycle is also independent of precession as that study suggests). Directly forced, nonlinear systems can have different modulation sensitivities depending on whether feedbacks in the climate system amplify (large sensitivity, positive feedbacks), suppress (small sensitivity, negative feedbacks), or respond proportionally to (sensitivity of ~1, weak feedbacks) changes in the amplitude of forcing.

Here we specifically consider the hypothesis of Ashkenazy and Tziperman (2004) that 41-kyr glacial cycles in the late Pliocene and early Pleistocene were generated by self-sustained variability. Their study demonstrates that a nonlinear sea-ice switch model (Gildor and Tziperman, 2000; Tziperman and Gildor, 2003) can produce asymmetric 41-kyr cycles with almost no obliquity forcing. A small obliquity term in the model constitutes 10% of the forcing in the ice-sheet mass balance equation and allows obliquity to control the timing of glacial terminations via the mechanism of nonlinear phase locking. The authors find that similar glacial cycles can also be produced when the model is driven by 21 June insolation at 65°N.

The 41-kyr sea-ice switch model has a modulation sensitivity of only 0.31 for the 41-kyr power of ice volume when driven by obliquity. When driven by insolation, the model's sensitivity to obliquity modulation is surprisingly high at 1.17. This is because when obliquity forcing is weak, the duration of glacial cycles becomes more variable due to the greater relative influence of precession. If the 41-kyr band is expanded to $1/55–1/38\,kyr^{-1}$, the modulation sensitivity of model response is reduced to 0.30. In contrast, expanding the frequency band for $\delta^{18}O$ response has little effect on its modulation sensitivity to obliquity, changing the average value from 1.20 to 1.05 for the interval 5.3–1.4 Myr. We conclude that the small modulation sensitivity to obliquity in the sea ice switch model is inconsistent with the climate's modulation sensitivity before 1.4 Myr. However, the initiation of self-sustained variability could be responsible for the near-zero modulation sensitivity to obliquity after 1.4 Myr.

For precession the modulation sensitivity of benthic $\delta^{18}O$ is 1.1 for the 19-kyr band and 1.8 for the 23-kyr band (Table 1). The different values for the two frequencies of precession are difficult to explain, but as previously noted, weak precession responses are much more susceptible to measurement error. Regardless, the correlation of power in forcing and detrended response (Fig. 4) and the modulation sensitivities greater than one confirm that precession responses are directly forced either linearly or with nonlinear positive feedbacks. This response is not consistent with pacing by precession or with nonlinear combination tones of 100- and 41-kyr cycles (unless the amplitude of 100-kyr response is affected by precession modulation).

5.2. Constraints of cycle shape

Changes in glacial shapes are diagnostic of a change in climate dynamics unless they are externally forced or result from systematic age model errors. As described in Section 4, no changes in the asymmetry or skewness of orbital forcing occur during the last 5 Myr. The artificial distortion of glacial cycle shapes by overtuning is ruled out because the same glacial shapes are observed in the untuned age model with constant average sedimentation rate (Figs. 6b and 7). The asymmetry of early Pleistocene cycles is also observed in other studies (Raymo, 1992; Ashkenazy and Tziperman, 2004; Huybers, 2007) using different age models and different methods of quantifying asymmetry. However, glacial cycle shapes in all of these age models could potentially be distorted if sedimentation rates varied consistently and globally on glacial–interglacial timescales.

For the following discussion changes in the shapes of glacial climate response are judged to be more likely than large, orbital-scale changes in global sedimentation rates. However, changes in cycle asymmetry or skewness resulting from changes in sedimentation rates would still be indicative of some change in climate dynamics.

The presence of asymmetry and/or skewness in glacial cycles over most of the climate record requires some nonlinearity in orbital responses throughout the Plio–Pleistocene. (Prior to 1 Myr this nonlinearity presumably applies to obliquity responses because 41-kyr power dominated the climate record.) Asymmetric responses to symmetric forcing are found in many nonlinear models of climate response. Ashkenazy and Tziperman (2004) attribute glacial asymmetry to self-sustained variability, but that model is inconsistent with the modulation sensitivity of obliquity responses before 1.4 Myr. In contrast, piecewise linear models (e.g., Imbrie and Imbrie, 1980; Paillard, 1998) can produce asymmetric responses that also exhibit a modulation sensitivity of ~1. Therefore, we propose that obliquity responses before 1.4 Myr are best described by piecewise linear climate models.

Several lines of evidence support the traditional view that saw-tooth asymmetry in glacial cycles is generated by different response times for the growth and decay of northern hemisphere ice sheets (e.g., Imbrie and Imbrie, 1980; Paillard, 1998; Clark et al., 1999). (i) The appearance of glacial asymmetry is approximately coeval with the onset of major northern hemisphere glaciation. (ii) Glacial asymmetry is observed before 1.4 Myr, while cycle amplitudes display a proportional response to obliquity modulation. (iii) Asymmetric responses are observed on both millennial (e.g., Grootes et al., 1993; MacAyeal, 1993) and orbital timescales. (iv) Glacial dynamics includes many mechanisms that allow for rapid ice sheet decay (e.g., Clark et al., 1999; Tarasov and Peltier, 2004), including basal sliding, iceberg calving, a nonlinear sensitivity to temperature, and a positive feedback with sea level. Conversely, long-term ice sheet growth is slowed by a negative feedback between ice sheet height and accumulation rate and by millennial-scale Heinrich and Dansgaard-Oeschger-like events (e.g., MacAyeal, 1993; Marshall et al., 2000), which have also been observed in 41-kyr glacial cycles (Raymo et al., 1998).

A piecewise linear climate response can also create skewness in glacial cycles. The large, positive skewness of $\delta^{18}O$ before ~1.4 Myr might result from a reduced sensitivity to insolation during interglacial conditions. For example, warm temperatures could prevent northern ice sheets from growing before high-latitude summer insolation falls below some critical threshold (Raymo, 1997), allowing interglacial conditions to persist for more than half of an obliquity cycle. Such rectification can create skewness in the $\delta^{18}O$ record with minimal disruption to modulation sensitivity. At about 1.4 Myr the relative duration of interglacial stages decreases and the skewness of glacial cycles becomes slightly negative. Because this change is approximately coeval with the sudden decline in modulation sensitivity to obliquity, it is likely the result of a significant change in climate dynamics.

Figs. 6 and 7 show the asymmetry and skewness generated by two piecewise linear models of ice volume (Imbrie and Imbrie, 1980; Paillard, 1998). Although these models generate nonlinear cycle shapes, a different model or set of parameterizations is needed to reproduce the asymmetry and skewness observed in the Plio–Pleistocene climate record.

We conclude that both the asymmetry and skewness of glacial cycles before 1.4 Myr are consistent with a piecewise linear climate response. Although, such a response is nonlinear, the glacial dynamics of the climate system do share some characteristics with a linear response, most notably a proportional response to changes in the power of orbital forcing. Because 41-kyr responses before 1.4 Myr and 23-kyr responses throughout the Plio–Pleistocene appear to be directly driven by orbital forcing, we conclude that the comparison of these responses with obliquity and precession forcing can be used reconstruct changes in climate sensitivity.

6. Trends and transitions

We find that global cooling, climatic variance, sensitivity to orbital forcing, and glacial asymmetry are all well described by long-term trends over most of the Plio–Pleistocene. The importance of long-term trends in the evolution of Plio–Pleistocene climate response is also supported by Huybers (2007) using a different $\delta^{18}O$ stack. The Huybers stack spans 2 Myr, is the average of 4–14 $\delta^{18}O$ records with a lower resolution alignment, and has an age model based solely on the assumption of constant average sedimentation rate between paleomagnetic age constraints. Using a 200-kyr sliding window, Huybers finds linear trends in the mean, standard deviation, asymmetry, and weighted average frequency of the 2-Myr $\delta^{18}O$ stack. Our results also show approximately linear trends in mean, variance, and asymmetry (measured with a different statistic) when examined over the last 2 Myr. However, we find that an exponential slope is necessary to describe the trend in $\delta^{18}O$ variance since 5 Myr. Exponential trends in obliquity and precession sensitivity despite a linear trend in mean $\delta^{18}O$ suggest that climate sensitivity to a range of forcings may be exponentially dependent on mean climate state.

Glacial cycle shapes and the power of obliquity and precession responses suggest two major transitions in climate system dynamics during the Plio–Pleistocene. However, the abruptness and exact timing of these transitions are not well constrained due to the relatively large window sizes necessary to compensate for signal noise and age model uncertainty. (One exception is the decrease in 41-kyr response relative to obliquity forcing, which occurs within a single obliquity cycle from 1.44 to 1.4 Myr.) The first major climate transition is approximately coeval with the

onset of major northern hemisphere glaciation (NHG) at ~2.7 Myr. The second and possibly more significant climate transition occurs in the early Pleistocene at ~1.4 Myr. The MPT to 100-kyr glacial cycles at ~0.8 Myr does not correspond to any large change in glacial cycle shape, obliquity response, or precession sensitivity.

6.1. Onset of Northern Hemisphere glaciation

Precession sensitivity and the asymmetry of glacial cycles begin to increase some time between 3 and 2.5 Myr, and the onset of major NHG occurs at ~2.7 Myr. Because glacial asymmetry, precession sensitivity, and the size of northern hemisphere ice sheets all begin increasing trends at ~2.7 Myr, the onset of NHG appears to be associated with the start of a gradual change in the dynamics of glacial cycles. We propose that glacial asymmetry and precession sensitivity are either controlled by the dynamics of the northern ice sheets directly or by the same factor which determines the glacial maximum in northern ice volume.

The fact that precession sensitivity begins to increase at ~2.7 Myr while obliquity continues along a single exponential trend from 5.3 to 1.4 Myr suggests that the dynamics of precession and obliquity response differ. Several studies (e.g., Philander and Fedorov, 2003; Raymo and Nisancioglu, 2003; Raymo et al., 2006; Huybers, 2006) have proposed disparate responses to precession and obliquity based on the particular effects they have on the seasonal and latitudinal distribution of insolation. Unlike obliquity, precession forcing is out-of-phase across hemispheres and acts only on the seasonal distribution of insolation, not the annual average. Obliquity and precession responses in benthic $\delta^{18}O$ may also differ in their ratios of ice volume change to deep water temperature change (e.g., Shackleton, 2000; Lisiecki and Raymo, 2005).

The correlation between northern hemisphere ice sheet size and precession sensitivity is consistent with any theory in which precession response scales with the overall variability of northern hemisphere ice volume. However, models must also explain the different trends in sensitivity for obliquity and precession. The piecewise linear models of Imbrie and Imbrie (1980) and Paillard (1998) cannot reproduce the climate's differential responses to obliquity and precession because they are forced by a single insolation curve. An additional level of complexity is required to capture this aspect of Plio–Pleistocene climate evolution.

Raymo et al. (2006) propose a model consistent with the observed trends in obliquity and precession sensitivity. In this model ice volume from each hemisphere responds to local insolation, creating out-of-phase precession responses during the Pliocene and early Pleistocene. Before the appearance of large northern hemisphere ice sheets, the out-of-phase precession responses in the north and south nearly balanced out, leaving the $\delta^{18}O$ record dominated by in-phase obliquity responses. As northern ice volume increased, it began to outweigh the compensating southern response, and precession power in the global climate signal also increased. In contrast, the obliquity responses recorded by $\delta^{18}O$ are in-phase across hemispheres. Therefore, the sum of northern and southern obliquity responses could follow one continuous exponential trend despite possible changes in the ratio of response across hemispheres.

6.2. Early Pleistocene transition

In this section we describe the changes observed in climate response at 1.4 Myr and discuss their implications for models of glacial cycle dynamics. The most convincing evidence for a substantial change in climate dynamics at 1.4 Myr is the switch from a directly forced obliquity response to a nonlinear one that is insensitive to obliquity modulation. Self-sustained variability paced by obliquity is one possible mechanism for generating the constant 41-kyr response after 1.4 Myr. As demonstrated in Section 5.1, the sea-ice switch model (Ashkenazy and Tziperman, 2004) is largely insensitive to the modulation of obliquity forcing.

Another change observed at 1.4 Myr is an abrupt decrease in the amplitude of 41-kyr response (not detrended, see Fig. 5b) while obliquity forcing is increasing. This suggests that the change in climate dynamics occurred rapidly and that the nonlinear 41-kyr responses after 1.4 Myr are weaker than the piecewise linear responses just before. In general, one might also expect a large change in 41-kyr dynamics to alter the phase of 41-kyr response relative to obliquity forcing. Response lags are difficult to estimate, but an abrupt shift in the relative phases of precession and obliquity is observed in $\delta^{18}O$ at ~1.4 Myr (Lisiecki and Raymo, 2005). The LR04 age model assumes that obliquity phase stays approximately constant at this time while precession lag increases rapidly. However, the changes in obliquity sensitivity at 1.4 Myr may better support an alternate age model in which precession lag remains constant and obliquity lag declines. The final change observed near 1.4 Myr is a step-like decrease in the skewness of glacial cycles. The timing of this event suggests that it is related to the change in 41-kyr dynamics and may be a useful statistic with which to evaluate models of obliquity response.

In summary, the change in glacial dynamics at ~1.4 Myr is associated with an abrupt decline in 41-kyr power, a decrease in modulation sensitivity to obliquity, and a decrease in the relative duration of interglacials. The phase of either precession or obliquity response may change at ~1.4 Myr, but sensitivity to precession continues its gradual increase. We suggest that future studies attempt to identify changes in the climate system at ~1.4 Myr in order to constrain the mechanisms which might be responsible for this transition in obliquity response.

6.3. Mid-Pleistocene transition

During the increase in 100-kyr power in the mid-Pleistocene, we observe no change in obliquity dynamics

or the skewness of glacial cycles and no change in the long-term trends of precession sensitivity or glacial asymmetry. Therefore, to be consistent with the climate record, models of the MPT must be able to reproduce these features.

One possible explanation for the approximately constant 41-kyr power in $\delta^{18}O$ over the last 1.4 Myr is that the dynamics controlling 41-kyr response are unrelated to those generating 100-kyr power since ~0.8 Myr (Fig. 2a). However, it is also possible to construct models in which 41-kyr cycles "transform" into quasi-100-kyr cycles without producing large changes in 41-kyr power. Ashkenazy and Tziperman (2004) propose that gradually declining temperatures produced a sudden shift to quasi-100-kyr cycles when the threshold for sea ice formation was reached every 2–3 obliquity cycles or 4–5 precession cycles. This model produces relatively constant 41-kyr power across the MPT when driven by pole-equator insolation gradients (dominated by obliquity) but not when driven by July insolation at 65°N. Huybers (2007) presents another model of orbital pacing in which quasi-100-kyr power increases gradually over the last 2 Myr as obliquity-paced terminations are "skipped" more frequently. This model also produces approximately constant 41-kyr power across the MPT.

Huybers (2007) supports the hypothesis of a gradual change in obliquity response with the identification of a linear, 2-Myr trend in the first moment of the power spectrum, M_1, which is a weighted average of response frequency. He suggests that this trend toward lower-frequency power results from long-term changes in the climate system such as cooling or ice sheet growth. However, we find two problems with this explanation of obliquity response change. First, a gradual shift in frequency response cannot explain why glacial cycles respond to obliquity modulation before 1.4 Myr but not after. (The Huybers model of obliquity pacing is insensitive to the modulation of obliquity forcing for all of the last 2 Myr.) Second, in the LR04 stack the trend in M_1 reverses at ~2 Myr due to the presence of low frequency power from 3.5 to 2.5 Myr. Therefore, the shift to lower frequencies in $\delta^{18}O$ from 2 to 0 Myr may not be a simple response to long-term cooling or ice sheet growth. We suggest that climate records spanning at least the last 3 Myr be used when interpretting the relationship between observed climate responses and the MPT.

Despite problems with the specific 2-Myr trend in obliquity response proposed by Huybers (2007), the spectral power and shape of glacial responses alone cannot determine whether groupings of obliquity cycles have produced the strong 100-kyr power of the late Pleistocene. Another metric, such as the timing of terminations relative to orbital forcing, is needed. Huybers and Wunsch (2005) demonstrate a correlation between the timing of late Pleistocene terminations and obliquity forcing, but age model uncertainties preclude an evaluation of the role of precession in pacing the 100-kyr cycle.

7. Conclusions

A comparison of climate responses with obliquity and precession forcing reveals several important trends and transitions in the climate system during the Plio–Pleistocene. Total variance in benthic $\delta^{18}O$ follows an exponential trend for the entire 5.3 Myr, but sensitivity to obliquity and precession forcing follow somewhat different trends. Precession response is directly forced over the entire 5.3-Myr period, but its exponential increase in sensitivity does not begin until ~2.5 Myr. Obliquity response appears directly forced with exponentially increasing sensitivity from 5.3 to 1.4 Myr, but after 1.4 Myr the 41-kyr power of glacial cycles becomes approximately constant and uncorrelated with modulations in obliquity forcing. Exponential trends in obliquity and precession sensitivity in conjunction with a linear trend in mean $\delta^{18}O$ suggest that climate sensitivity to a range of forcings may be exponentially dependent on mean climate state.

Quantitative descriptions of glacial cycle shape demonstrate that the saw-tooth asymmetry of glacial cycles first appears at ~2.5 Myr and then gradually increases. The skewness of $\delta^{18}O$ displays a step-like decrease at 1.4 Myr, indicating a decrease in the relative duration of interglacial conditions. Overall, climate responses to obliquity and precession in the Plio–Pleistocene appear to follow steady trends with transitions at approximately 2.5 and 1.4 Myr. No abrupt transition in glacial cycle shape or in obliquity and precession responses is observed during the appearance of 100-kyr cycles at ~0.8 Myr.

The observations of climate response presented in this study have implications for the numerous models that have been proposed to explain glacial dynamics and Plio–Pleistocene climate transitions. We find that glacial responses before 1.4 Myr are most consistent with piecewise linear models (e.g., Imbrie and Imbrie, 1980; Paillard, 1998) and suggest that future models explicitly include either the spatial or seasonal distribution of insolation to account for the different trends in obliquity and precession sensitivity over the Plio–Pleistocene. Models invoking self-sustained variability paced by obliquity (e.g., Ashkenazy and Tziperman, 2004; Huybers, 2007) may explain the lack of correlation in the 41-kyr power of forcing and response after 1.4 Myr. However, our observations cannot determine whether late Pleistocene 100-kyr power results from groupings of 2–3 obliquity cycles. To be consistent with the climate record, models of the MPT should produce no large change in 41-kyr climate response or cycle skewness after ~1.4 Myr and no change in the long-term trend of precession sensitivity. We encourage future models of Plio–Pleistocene transitions to be evaluated with respect to changes in glacial cycle shape and response power relative to orbital forcing throughout the last 5 Myr.

Acknowledgments

We thank all of the researchers who have made their data available for the benthic stack; without their work,

these results would not be possible. E. Tziperman, P. Huybers, Z. Liu, K. Lawrence, and L. Cleaveland also contributed many helpful comments regarding this manuscript. L. Lisiecki also thanks T. Herbert, W. Prell, and S. Clemens for their advice and guidance. L. Lisiecki is supported by the NOAA Postdoctoral Program in Climate and Global Change, administered by the University Corporation for Atmospheric Research. M. Raymo acknowledges the support of NSF Grant ATM-0220681.

References

Ashkenazy, Y., Tziperman, E., 2004. Are the 41 kyr glacial oscillations a linear response to Milankovitch forcing? Quaternary Science Reviews 23, 1879–1890.

Berger, A., Li, X.S., Loutre, M.F., 1999. Modeling northern hemisphere ice volume over the last 3 Myr. Quaternary Science Reviews 18, 1–11.

Cane, M.A., Molnar, P., 2001. Closing of the Indonesian seaway as a precursor to east African aridification around 3–4 million years ago. Nature 411, 157–162.

Clark, P.U., Pollard, D., 1998. Origin of the middle Pleistocene transition by ice sheet erosion of regolith. Paleoceanography 13, 1–9.

Clark, P.U., Alley, R.B., Pollard, D., 1999. Northern hemisphere ice-sheet influences on global climate change. Science 286, 1104–1111.

Denton, G.H., Alley, R.B., Comer, G.C., Broecker, W.S., 2005. The role of seasonality in abrupt climate change. Quaternary Science Reviews 24, 1159–1182.

Gildor, H., Tziperman, E., 2000. Sea ice as the glacial cycles climate switch: role of seasonal and orbital forcing. Paleoceanography 15, 605–615.

Grootes, P.M., Stuvier, M., White, J.W.C., Johnsen, S.J., Jouzel, J., 1993. Comparison of oxygen isotope records from GISP2 and GRIP Greenland ice cores. Nature 366, 552–554.

Hagelberg, T.K., Pisias, N., Edgar, S.L., 1991. Linear and nonlinear couplings between orbital forcing and the marine $\delta^{18}O$ record during the late Neogene. Paleoceanography 6, 729–746.

Haug, G.H., Tiedemann, R., 1998. Effect of the formation of the Isthmus of Panama on Atlantic Ocean thermohaline circulation. Nature 393, 673–676.

Haug, G.H., Sigman, D.M., Tiedemann, R., Pedersen, T.F., Sarnthein, M., 1999. Onset of permanent stratification in the subarctic Pacific Ocean. Nature 401, 779–782.

Huybers, P., 2006. Early Pleistocene glacial cycles and the integrated summer insolation forcing. Science 313, 508–511.

Huybers, P. 2007 Glacial variability over the last two million years: an extended depth-derived agemodel, continuous obliquity pacing, and the Pleistocene progression. Quaternary Science Reviews this issue, doi:10.1016/j.quascirev.2006.07.005.

Huybers, P., Wunsch, C., 2004. A depth-derived Pleistocene age model: uncertainty estimates, sedimentation variability, and nonlinear climate change. Paleoceanography 19, 1.

Huybers, P., Wunsch, C., 2005. Obliquity pacing of the late Pleistocene glacial terminations. Nature 434, 491–494.

Imbrie, J., Imbrie, J.Z., 1980. Modeling the climatic response to orbital variations. Science 207, 943–953.

Imbrie, J., Hays, J.D., Martinson, D.G., McIntyre, A., Mix, A.C., Morley, J.J., Pisias, N.G., Prell, W.L., Shackleton, N.J., 1984. The orbital theory of Pleistocene climate: support from a revised chronology of the marine $\delta^{18}O$ record. In: Berger, A. (Ed.), Milankovitch and Climate, Part 1. D. Reidel, Hingham, MA, pp. 269–305.

Imbrie, J., Boyle, E.A., Clemens, S.C., Duffy, A., Howard, W.R., Kukla, G., Kutzbach, J., Martinson, D.G., McIntyre, A., Mix, A.C., Molfino, B., Morley, J.J., Peterson, L.C., Pisias, N.G., Prell, W.L., Raymo, M.E., Shackleton, N.J., Toggweiler, J.R., 1992. On the structure and origin of major glaciation cycles, 1: linear responses to Milankovitch Forcing. Paleoceanography 7, 701–738.

Keigwin, L., 1982. Isotopic paleoceanography of the Caribbean and east Pacific: role of Panama uplift in late Neogene time. Science 217, 350–353.

King, T., 1996. Quantifying nonlinearity and geometry in the time series of climate. Quaternary Science Reviews 15, 247–266.

Laskar, J., Joutel, F., Boudin, F., 1993. Orbital, precessional and insolation quantities for the Earth from −20 Myr to +10Myr. Astronomy and Astrophysics 270, 522–533.

Lisiecki, L.E., Lisiecki, P.A., 2002. Application of dynamic programming to the correlation of paleoclimate records. Paleoceanography 17, 1049.

Lisiecki, L.E., Raymo, M.E., 2005. A Pliocene–Pleistocene stack of 57 globally distributed benthic $\delta^{18}O$ records. Paleoceanography 20, PA1003.

Liu, Z., Herbert, T.D., 2004. High-latitude influence on the eastern equatorial Pacific climate in the early Pleistocene epoch. Nature 427, 720–723.

MacAyeal, D.R., 1993. Binge/purge oscillations of the Laurentide Ice Sheet as a cause of the North Atlantic's Heinrich events. Paleoceanography 8, 775–784.

Maier-Reimer, E., Mikolajewicz, U., Crowley, T.J., 1990. Ocean general circulation model sensitivity experiment with an open American Isthmus. Paleoceanography 5, 349–366.

Marshall, S.J., Tarasov, L., Clarke, G.K.C., Peltier, W.R., 2000. Glaciological reconstruction of the Laurentide Ice Sheet: physical processes and modelling challenges. Canadian Journal of Earth Science 37, 769–793.

Maslin, M.A., Li, X.S., Loutre, M.-.F., Berger, A., 1998. The contribution of orbital forcing to the progressive intensification of Northern Hemisphere glaciation. Quaternary Science Reviews 17, 411–426.

Paillard, D., 1998. The timing of Pleistocene glaciations from a simple multiple-state climate model. Nature 391, 378–381.

Philander, S.G., Fedorov, A.V., 2003. Role of tropics in changing the response to Milankovitch forcing some three million years ago. Paleoceanography 18, PA1045.

Ravelo, A.C., Andreasen, D.H., Lyle, M., Lyle, A.O., Wara, M.W., 2004. Regional climate shifts caused by gradual cooling in the Pliocene epoch. Nature 429, 263–267.

Raymo, M.E., 1992. Global climate change: a 3 million year perspective. In: Kukla, G., Went, E. (Eds.), Start of a Glacial, NATO ASI Series I, vol. 3, Proceedings of the Mallorca NATO ARW. Springer, Heidelberg, pp. 207–223.

Raymo, M.E., 1997. The timing of major climate terminations. Paleoceanography 12, 577–585.

Raymo, M.E., Nisancioglu, K., 2003. The 41 kyr world: Milankovitch's other unsolved mystery. Paleoceanography 18, PA1011.

Raymo, M.E., Ruddiman, W.F., Froelich, P.N., 1988. Influence of late Cenozoic mountain building on ocean geochemical cycles. Geology 16, 649–653.

Raymo, M.E., Ganley, K., Carter, S., Oppo, D.W., McManus, J., 1998. Millenial-scale climate instability during the early Pleistocene epoch. Nature 392, 699–702.

Raymo, M.E., Lisiecki, L.E., Nisancioglu, K.H., 2006. Plio–Pleistocene ice volume, Antarctic climate, and the global $\delta^{18}O$ record. Science 313, 492–495.

Rea, D.K., Snoeckx, H., Joseph, L.H., 1998. Late Cenozoic eolian deposition in the North Pacific: Asian drying, Tibetan uplift, and cooling of the Northern Hemisphere. Paleoceanography 13, 215–224.

Shackleton, N.J., 1995. New data on the evolution of Pliocene climate variability. In: Vrba, E.S., et al. (Eds.), Paleoclimate and Evolution, With Emphasis on Human Origins. Yale University Press, New Haven, CT, pp. 242–248.

Shackleton, N.J., 2000. The 100,000-year ice-age cycle identified and found to lag temperature, carbon dioxide, and orbital eccentricity. Science 289, 1897–1902.

Sigman, D.M., Jaccard, S.L., Haug, G.H., 2004. Polar stratification in a cold climate. Nature 428, 59–63.

Tarasov, L., Peltier, W.R., 2004. A geophysically constrained large ensemble analysis of the deglacial history of the North American ice-sheet complex. Quaternary Science Reviews 23, 359–388.

Tiedemann, R., Sarnthein, M., Shackleton, N.J., 1994. Astronomic timescale for the Pliocene Atlantic $\delta^{18}O$ and dust flux records of Ocean Drilling Program site 659. Paleoceanography 9, 619–638.

Tziperman, E., Gildor, H., 2003. On the mid-Pleistocene transition to 100-kyr glacial cycles and the asymmetry between glaciation and deglaciation times. Paleoceanography 18.